Asymmetric interactive buckling of thin-walled columns with initial imperfections

Marcello Pignataro, Angelo Luongo

Asymmetric Interactive Buckling of Thin-Walled Columns with Initial Imperfections

M. Pignataro and A. Luongo

Dip. Ingegneria Strutturale e Geotecnica, Università di Roma 'La Sapienza', Rome, Italy

ABSTRACT

In this paper the effect of the interaction between two or more simultaneous buckling modes on the postbuckling behaviour of uniformly compressed thin-walled members (TWM) is analysed by means of the general theory of elastic stability. The analysis is restricted to third-order terms of the energy expansion and therefore can be fruitfully applied to the investigation of structures with asymmetric postbuckling behaviour only. Initial imperfection effect is taken into account. A simplified procedure is suggested for solving the nonlinear equations relative to the evaluation of the bifurcated paths. By using the finite strip method an extensive parametric analysis is performed. It is found that when the flexural–torsional (FT) buckling interacts with a local symmetric and antisymmetric mode, sensitivity to initial imperfections is remarkable and is comparable to the one arising from the interaction between the Euler (E) and any local buckling.

1 INTRODUCTION

The local and overall interaction buckling of elastic columns has extensively been investigated in the field of cold formed steel structures. There exist a number of significant papers on the subject which follow two different approaches:

(i) Post-local buckling analysis is first performed and then overall buckling is evaluated accounting for the reduction of the flexural stiffnesses.

(ii) Analysis of the postbuckling interaction is performed on the basis of the general Koiter[1] theory.

Under the first category fall the papers by Wang and Pao,[2] Hancock,[3,4] Bradford and Hancock[5] who make use of the concept of the effective width to account for the postbuckling strength of the locally buckled component plates. Both the empirical formula suggested by Winter and a nonlinear finite strip analysis are employed.

The second approach is followed by Byskov and Hutchinson,[6] Sridharan *et al.*,[7-10] Pignataro *et al.*[11] In Ref. 6 a reformulation of Koiter's theory on the basis of the virtual work principle is proposed and general equilibrium equations for single, simultaneous and nearly simultaneous buckling modes are furnished. These equations are utilised in Refs. 7–10 in conjunction with an innovative combination of the finite strip and finite element techniques and are solved numerically for the case of nearly simultaneous modes in the presence of initial imperfections. A similar approach is followed in Ref. 11 where a nontraditional finite strip technique has been developed through an automatic procedure of algebraic manipulation.

In all previous works interaction between two buckling modes only has been considered (single interaction). In a few recent papers[12,13] the problem of multiple interaction involving an overall mode and several local modes has been investigated.

In this paper a third-order analysis suitable for structures with asymmetric postbuckling behaviour is performed on the basis of Koiter's theory. It is assumed that two (or more) buckling modes interact simultaneously. Initial imperfections in the shape of the buckling mode associated with the bifurcated path of steepest descent are considered. This permits the avoidance of the numerical solution of a nonlinear system by solving a single equation in closed form. A simplifying procedure has been successively developed on the basis of sound physical assumptions which permit the replacement of the nonlinear equilibrium system by a linear eigenvalue problem.

A number of numerical results regarding angle sections and channels simply supported at the ends under uniform compression have been obtained. In contrast with previous achievements it is shown that local-FT interaction can be equally detrimental as the local-E one whenever two local modes are present, the one symmetric, the other one antisymmetric.

2 STRUCTURAL MODEL AND POSTBUCKLING ANALYSIS

Let us consider the TWM as a plate assemblage and refer to a single plate of length l, width b and thickness t uniformly compressed by the stress N_x in the

longitudinal direction x. The total potential energy is then

$$\phi = \frac{Et}{2(1-\nu^2)} \int_0^b \int_0^l \left[\epsilon_x^2 + \epsilon_y^2 + 2\nu\epsilon_x\epsilon_y + \frac{1}{2}(1-\nu)\gamma_{xy}^2 \right] dx\,dy$$

$$+ \frac{Et^3}{24(1-\nu^2)} \int_0^b \int_0^l \left[\chi_x^2 + \chi_y^2 + 2\nu\chi_x\chi_y + \frac{1}{2}(1-\nu)\chi_{xy}^2 \right] dx\,dy$$

$$- \lambda \int_0^b N_x[u(0,y) - u(l,y)]\,dy \tag{1}$$

where E is the Young's modulus, ν the Poisson's ratio and λ a load parameter. For the strain measures we assume

$$\epsilon_x = u_{,x} + \frac{1}{2}(v_{,x}^2 + w_{,x}^2) \qquad \chi_x = w_{,xx}$$

$$\epsilon_y = v_{,y} + \frac{1}{2}(u_{,y}^2 + w_{,y}^2) \qquad \chi_y = w_{,yy} \tag{2}$$

$$\gamma_{xy} = u_{,y} + v_{,x} + w_{,x}w_{,y} \qquad \chi_{xy} = 2w_{,xy}$$

where u, v are the in-plane displacement components in the x, y directions, and w is the lateral displacement.

If initial imperfections $\bar{u}, \bar{v}, \bar{w}$ are present and assuming the plate to be stress free in the imperfect unloaded state, the total potential energy ϕ is modified by the addition of the extra contribution

$$\psi = -\frac{Et}{1-\nu^2} \int_0^b \int_0^l \left[u_{,x}\bar{u}_{,x} + \nu(u_{,x}\bar{v}_{,y} + \bar{u}_{,x}v_{,y}) + v_{,x}v_{,y} \right.$$

$$\left. + \frac{1-\nu}{2}(u_{,y} + v_{,x})(\bar{u}_{,y} + \bar{v}_{,x}) \right] dx\,dy$$

$$- \frac{Et^3}{12(1-\nu^2)} \int_0^b \int_0^l [w_{,xx}\bar{w}_{,xx} + \nu(w_{,xx}\bar{w}_{,yy} + \bar{w}_{,xx}w_{,yy})$$

$$+ w_{,yy}\bar{w}_{,yy} + 2(1-\nu)w_{,xy}\bar{w}_{,xy}]\,dx\,dy \tag{3}$$

where only linear terms in the initial displacements have been retained. The total energies Φ and Ψ of the TWM are obtained by summing all contributions (1), (3) from single plates.

To study the postbuckling behaviour of the perfect structure we express the bifurcated path $\mathbf{v} = \mathbf{v}(\lambda)$ by a series expansion in terms of a parameter ξ[14]

$$\lambda = \lambda_c + \lambda_1 \xi + \ldots$$
$$\mathbf{v} = \mathbf{v}_1 \xi + \frac{1}{2}\mathbf{v}_2 \xi^2 + \ldots \tag{4}$$

where λ_c is the critical load and $\mathbf{v}$ is a displacement vector measured from the fundamental path. The coefficients of the series expansions (4) are determined by solving an eigenvalue problem and a second-order perturbation equation. In the case of r buckling modes $\mathbf{v}_{1i}$ associated with the same value λ_c we have for the general solution to the eigenvalue problem $\mathbf{v}_1 = \nu_i \mathbf{v}_{1i}$ where the summation convention with respect to repeated indices has been adopted. Without any loss in generality these modes can be orthonormalised according to $\Pi_2'' \mathbf{v}_{1i}\mathbf{v}_{1j} = \delta_{ij}$, where δ_{ij} is the Kronecker delta and Π_2'' collects all quadratic terms of the elastic contribution to the potential energy Φ. By requesting $\Pi_2'' \mathbf{v}_1^2 = 1$ the condition $\nu_i \nu_i = 1$ follows. The coefficients ν_i and λ_1 are determined by the nonlinear system

$$A_{ijk}\nu_i\nu_j + \lambda_1 B_{ik}\nu_i = 0 \quad (i,j,k = 1, \ldots, r) \tag{5}$$

where

$$A_{ijk} = \Phi_c'''\mathbf{v}_{1i}\mathbf{v}_{1j}\mathbf{v}_{1k} \quad B_{ik} = 2\dot{\Phi}_c''\mathbf{v}_{1i}\mathbf{v}_{1k} \tag{6}$$

a prime denoting Fréchet differentiation and $\dot{\Phi}_c'' = [\mathrm{d}\Phi''/\mathrm{d}\lambda]_{\lambda=\lambda_c}$.

For the analysis of the imperfect structure we assume for the initial displacements $\bar{\mathbf{u}} = \bar{\xi}\mathbf{u}^*$ where $\bar{\xi}$ is the amplitude and $\mathbf{u}^*$ denotes the imperfection shape which is selected as $\mathbf{u}^* = \nu_i^* \mathbf{v}_{1i}$, ν_i^* being the set of coefficients corresponding to the postbuckling path of steepest descent of the perfect structure. In this case the snapping load is furnished by

$$\frac{\lambda_s}{\lambda_c} = 1 - 2\sqrt{-\frac{\bar{\xi}\rho\lambda_1^*}{\lambda_c}} \tag{7}$$

for $\lambda_1^* > 0$ and $\rho\bar{\xi} < 0$ or vice versa. In eqn (7) $\lambda_1^* = \max|\lambda_1|$ and $\rho = \tilde{\Psi}_c'(\nu_i^*\mathbf{v}_{1i})^2/\lambda_c\Phi_c''(\nu_i\mathbf{v}_{1i})^2$ where a tilde denotes differentiation with respect to $\bar{\mathbf{u}}$.

For a TWM, under the assumption of free transverse expansion, one obtains $B_{ij} = -2\delta_{ij}/\lambda_c$ and $\rho = 1$. By eliminating ξ from eqns (4) the equilibrium path is obtained

$$\frac{\lambda}{\lambda_c} = 1 + \mu\frac{\nu_P}{h} \tag{8}$$

where

$$\mu = \frac{\lambda_1}{\lambda_c} \frac{h}{\nu_i^* \nu_{1i}^P}$$

ν_P being a displacement component of a selected point P of the TWM, ν_{1i}^P the contribution to ν_P from the ith buckling mode, and h a dimension of the cross-section. The snapping load (7) simplifies to

$$\frac{\lambda_s}{\lambda_c} = 1 - 2\sqrt{-\mu \frac{\bar{u}_P}{h}} \tag{10}$$

where $\bar{u}_P$ is a component of the displacement of the point P due to initial imperfections.

3 SIMPLIFIED ANALYSIS

Let us consider the case of multiple interaction between one overall mode (Eulerian or flexural–torsional) and m local modes and assume that (i) in the local modes joints do not translate so that only lateral displacements of the plate components are possible, (ii) in the overall mode the TWM buckles as a shear indeformable beam with free transverse expansion. Then, by referring indices $i = 1$ to overall mode and $i > 1$ to local modes, $A_{ijk} = 0$ for $i, j, k > 1$ and

$$A_{1jk} = \int_S Et(u_{1,x} w_{j,x} w_{k,x}) \mathrm{d}S \qquad (j,k = 1,2,\ldots,m+1) \tag{11}$$

where S is the middle surface of the TWM. Under the assumption that the displacement functions are described by sinusoidal laws in the longitudinal direction (simply supported edges with free warping) the dominant coefficients obtained by eqn (11) are those for which the number of longitudinal halfwaves n_j is of the order of n_k. For $|n_j - n_k| \gg 0$ the corresponding coefficients are much smaller and in particular they can be neglected if they are of the type A_{11k}, for $n_k \gg 1$. Equations (5) then simplify to

$$A_{1jk} \nu_j \nu_k - 2\frac{\lambda_1}{\lambda_c} \nu_1 = 0 \tag{12}_1$$

$$(A_{1jk} - \delta_{jk}\eta)\nu_k = 0 \quad (j,k = 2,3,\ldots m+1) \tag{12}_2$$

where

$$\eta = \frac{\lambda_1}{\nu_1 \lambda_c} \tag{13}$$

Note that $A_{111} = 0$ because of hypothesis (ii).

Equation $(12)_2$ is a linear eigenvalue problem whose solution furnishes m real eigenvalues. Denoting by $\eta_h, \nu_k^{(h)}$ the hth solution, the corresponding values of $\nu_1^{(h)}$ and $\lambda_1^{(h)}$ can be obtained by solving eqns $(12)_1$ and (13) giving

$$\nu_1^{(h)} = \frac{1}{\sqrt{3}}, \qquad \frac{\lambda_1^{(h)}}{\lambda_c} = \frac{\eta_h}{\sqrt{3}} \tag{14}$$

As a first illustration of the theory let us consider the case of simple interaction ($m = 1$). Equation $(12)_2$ furnishes $\eta = A_{122}$ and therefore from eqns (14) and (11) the simple formula

$$\frac{\lambda_1}{\lambda_c} = \frac{Et}{\sqrt{3}} \int_S u_{1,x} w_{2,x}^2 \, dS \tag{15}$$

follows with $\nu_2 = \pm\sqrt{2/3}$. The coefficients ν_i obtained in this case show that, along the bifurcated path, $\frac{1}{3}$ of the energy $\Pi_2'' \nu_1^2$ is associated with the overall mode and $\frac{2}{3}$ with the local mode. This comes from the fact that the buckling modes have been orthonormalised with respect to the quadratic operator Π_2''.

If the cross-section has one axis of symmetry, $u_{1,x}$ is a symmetric or antisymmetric function according to whether the overall buckling is Eulerian or flexural–torsional, respectively. Consequently $\lambda_1/\lambda_c \neq 0$ in the E-local interaction and $\lambda_1/\lambda_c = 0$ in the FT-local interaction both for symmetric and antisymmetric local modes.

As a second illustration of the theory let us now examine the case of the overall–local–local buckling interaction. The eigenvalue problem $(12)_2$ is

$$\begin{bmatrix} A_{122} - \eta & A_{123} \\ A_{123} & A_{133} - \eta \end{bmatrix} \begin{Bmatrix} \nu_2 \\ \nu_3 \end{Bmatrix} = \begin{Bmatrix} 0 \\ 0 \end{Bmatrix} \tag{16}$$

which leads to the following cases:

(i) $A_{123} \neq 0$, the three buckling modes are coupled and there are two postbuckling equilibrium paths;

(ii) $A_{123} = 0$, $A_{122} \neq A_{133} \neq 0$, the overall mode couples with the local mode 2 or 3 and two postbuckling paths occur with $(\lambda_1/\lambda_c)_{max} = \max(A_{122}, A_{133})/\sqrt{3}$;

(iii) $A_{123} = 0, A_{122} = A_{133} \neq 0$, the three buckling modes are coupled and there are an infinite number of postbuckling paths since in our approximate analysis the ratio ν_2/ν_3 is indeterminate;

(iv) $A_{123} = A_{122} = A_{133} = 0$, third-order analysis furnishes $\lambda_1/\lambda_c = 0$ and postbuckling paths can be determined only by fourth-order analysis.

TABLE 1
Coefficients A_{ijk} for Overall-local Interaction

Overall modes	*Local modes*			
	Any	*Symm.-symm.*	*Symm.-ant.*	*Ant.-ant.*
Eulerian	$A_{122} \neq 0$ $A_{133} \neq 0$	$A_{123} \neq 0$	$A_{123} = 0$	$A_{123} \neq 0$
Flex.-tors.	$A_{122} = 0$ $A_{133} = 0$	$A_{123} = 0$	$A_{123} \neq 0$	$A_{123} = 0$

If the cross-section has one axis of symmetry, one can easily show by using eqn (16) and invoking geometric considerations that the coefficients A_{ijk} take the values displayed in Table 1. It is apparent that Euler buckling can interact with two local modes both symmetric or antisymmetric. On the other hand the flexural–torsional mode interacts only with a symmetric and an antisymmetric local mode. In this case $\lambda_1/\lambda_c = \pm A_{123}/\sqrt{3}$ and $\nu_3 = \pm \nu_2 = \pm 1/\sqrt{3}$. It should be borne in mind, however, that A_{123} is very small if $|n_2 - n_3| >> 0$ and consequently the coupling is weak.

4 DISCRETE MODEL

A thin-walled member can be considered as a prismatic shell made of plates (finite strips) rigidly connected along nodal lines which are assumed continuously supported at the ends. By introducing an orthogonal cartesian reference frame X, Y, Z with the X-axis parallel to the nodal lines, we may describe the position of the generic nth nodal line by assigning the displacement components $U_n(X), V_n(X), W_n(X)$ in the X, Y, Z directions, respectively, and the rotation $\Theta_n(X)$. In order to obtain a discrete solution to our analysis we express these functions as series expansions suitable to satisfy the end conditions

$$U_n(x) = \sum_{k=1}^{r} U_{nk} \cos k\frac{\pi x}{l}, \quad V_n(x) = \sum_{k=1}^{r} V_{nk} \sin k\frac{\pi x}{l}$$

$$W_n(x) = \sum_{k=1}^{r} W_{nk} \sin k\frac{\pi x}{l}, \quad \Theta_n(x) = \sum_{k=1}^{r} \Theta_{nk} \sin k\frac{\pi x}{l} \tag{17}$$

having assumed that the X and x coordinates coincide.

Let us now consider the generic finite strip and express the local

displacement components as a function of the local nodal parameters through the relationships

$$u^e(x,y) = \sum_{k=1}^{r} [f_1(y)u_{1k} + f_2(y)u_{2k}]\cos k\frac{\pi x}{l}$$

$$v^e(x,y) = \sum_{k=1}^{r} [f_1(y)v_{1k} + f_2(y)v_{2k}]\sin k\frac{\pi x}{l} \tag{18}$$

$$w^e(x,y) = \sum_{k=1}^{r} [f_3(y)w_{1k} + f_4(y)\theta_{1k} + f_5(y)w_{2k} + f_6(y)\theta_{2k}]\sin k\frac{\pi x}{l}$$

In eqns (18) the $f_i(y)$'s ($i = 1, \ldots, 6$) are linear or cubic polynomials and the coefficients u_{1k}, v_{1k}, . . ., θ_{2k} represent the displacement amplitudes along the longitudinal sides of the strip associated with the kth harmonic. The strip displacement parameters $\{u_k\} = \{u_{ik}\, v_{ik}\, w_{ik}\, \theta_{ik}\}^T$ ($i = 1, 2$) are correlated with those of the adjacent nodal lines $\{U_k\} = \{U_{nk}\, V_{nk}\, W_{nk}\, \Theta_{nk}\}^T$ through the relationship $\{u_k\} = [R]\{U_k\}$ where $[R]$ is the rotation matrix. This permits one to ensure compatibility between the plate edges and the nodal lines. By introducing eqns (18) into eqns (1) and (3) through the kinematic relationships (2) and summing the contributions from all strips the discretised counterparts of the functionals Φ_c'' appearing in the eigenvalue problem and of Φ_c''' are obtained in terms of the nodal parameters.

5 NUMERICAL RESULTS

The finite strip method has been utilised to investigate the critical and postcritical behaviour of simply supported stiffened angle sections and channels under uniform compression. Figure 1 shows the cross-sections of the TWM investigated, whose geometry is described by the dimensionless parameters

$$\alpha = \frac{l}{h}, \quad \beta = \frac{b}{h}, \quad \gamma = \frac{t}{h}, \quad \delta = \frac{d}{h} \tag{19}$$

l being the TWM length.

In what follows we define the critical stress

$$\sigma_c = k\frac{\pi^2}{12}\frac{E}{1-\nu^2}\gamma^2 \tag{20}$$

where, in general, k depends on the four parameters (19). Besides, for the evaluation of the slope μ of the bifurcated path, the displacement v_P

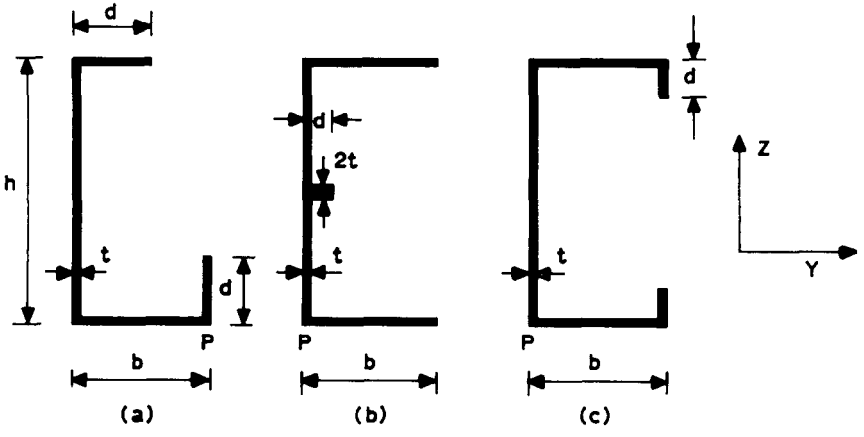

Fig. 1. Cross-sections geometry.

appearing in eqn (8) is identified with the displacement of point P (Fig. 1) in the Z-direction for the angle section and in the Y-direction for the channels.

5.1 Stiffened angle section

Figure 2 shows the dependence of k on c/h for an angle section with $\beta = 0{\cdot}6$ and $\gamma = 0{\cdot}01$ for different values of δ, c being the halfwavelength of the local buckling mode. It is seen that the curves for δ larger than a certain value, exhibit a minimum around $c/h = 1$ corresponding to the lowest local buckling. The overall critical stress is obtained by correspondence of $c = l$ and it is, in general, of the flexural–torsional type. As $l \to \infty$ it approaches zero and becomes of the Euler type. It may happen that for a TWM of fixed length for increasing δ overall critical stress is first smaller, then equal and finally larger than the local critical stress. Figure 3 shows the dependence of k on δ for $\gamma = 0{\cdot}01$ and a number of values of β and α. The three rising paths refer to the overall buckling (flexural–torsional). The relevant critical stress depends essentially on α, while the dependence on β is restricted within the narrow dashed areas ($0{\cdot}3 \leq \beta \leq 1$). The three nearly horizontal curves describe the local buckling whose critical stress is independent of α. Points of intersections of the two families of curves characterise interaction.

Table 2 collects results relative to postbuckling analysis and furnishes the values of the slope μ of the bifurcated path (eqn (8)). Results of the second last column have been obtained by solving the nonlinear eqn (5) where all coefficients have been calculated by means of the finite strip technique. By using the approximate formulae (12) the last column results are derived. It is seen that the largest difference between 'exact' and 'approximate' results

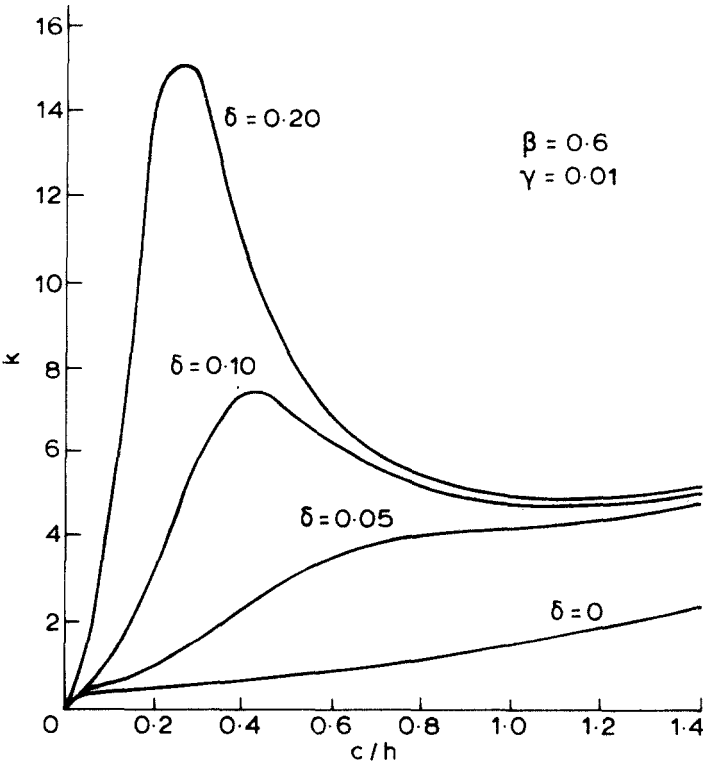

Fig. 2. Angle section: critical stress versus dimensionless wavelength.

TABLE 2
Angle Section: FT-local Interaction ($\gamma = 0{\cdot}01$)

	δ	α	$10^3\sigma_c/E$	ν_1	ν_2	μ	
						Eqn (5)	*Eqn (12)*
$\beta = 0{\cdot}3$	0·15	6·2	0·460	0·560	±0·828	10·108	9·853
	0·30	13·5	0·447	0·529	±0·842	2·971	2·923
$\beta = 0{\cdot}6$	0·15	6·5	0·446	0·555	±0·832	5·402	5·302
	0·30	14·0	0·442	0·536	±0·844	1·432	1·447
$\beta = 1{\cdot}0$	0·15	6·9	0·380	—	—	—	—
	0·30	15·5	0·375	0·572	±0·820	0·000 2	0·000 2

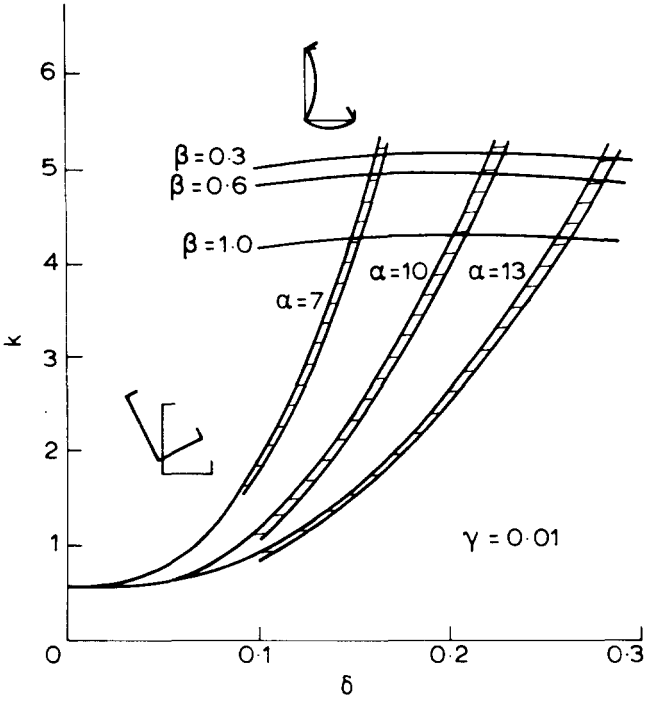

Fig. 3. Angle section: critical stress versus stiffener rigidity.

does not exceed 3% and therefore approximate theory can be used for practical purposes. This is also apparent from the values of ν_1 which are nearly constant and approximately equal to $\frac{1}{3}$.

By table inspection one can see that for increasing β, μ decreases and approaches zero for $\beta = 1$ (symmetric cross-section) according to previous qualitative analysis (Section 3). Note that for $\beta = 1$, $\delta = 0{\cdot}15$, $\alpha = 6{\cdot}9$ there is no coupling. Finally in Fig. 4 the snapping load λ_s against the initial imperfections amplitude $\bar{u}_P/h$ has been plotted. It is apparent that the more asymmetric the cross-section the higher the sensitivity to initial imperfections.

5.2 Stiffened channel: single interaction

In a previous work[15] the buckling behaviour of lipped and web-reinforced channels has been investigated. By inspection of qualitative results relative to local buckling (Fig. 5) one can see that, according to the size of the stiffeners, single and multiple interactions may occur both for symmetric and antisymmetric local buckling.

Results relative to FT-local interaction show that the slope of the

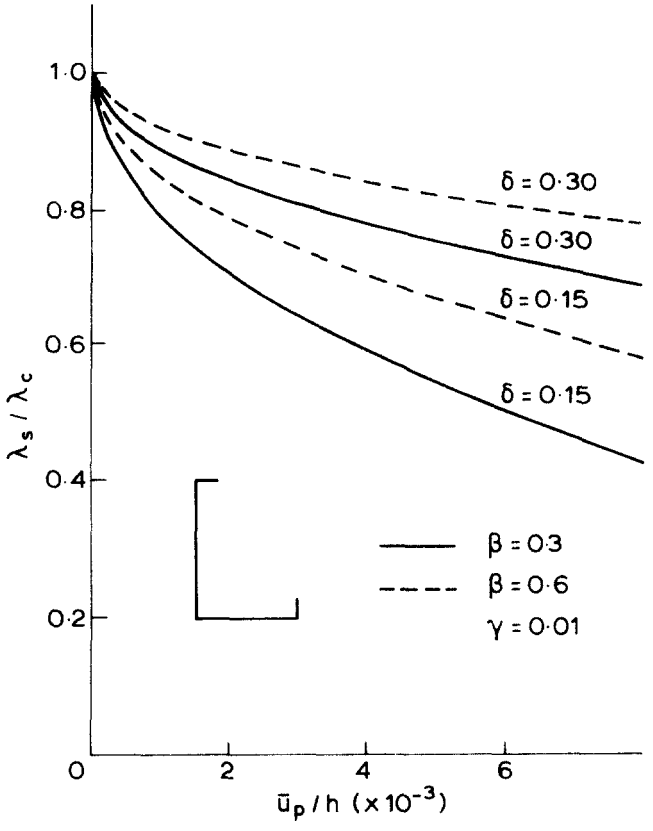

Fig. 4. Angle section: snapping load versus initial imperfection amplitude.

bifurcated path is approximately zero according to simplified analysis. On the other hand the E-local interaction is responsible for high imperfection sensitivity. This is apparent from Tables 3 and 4 where numerical results are displayed. In Table 3, relative to E-local interaction for a web-stiffened channel, it is noted that there is a jump in the value of μ from 1·35 to 14·56 when the local mode changes from symmetric into antisymmetric around $\delta = 0{\cdot}06$. The slopes of the equilibrium paths of the unstiffened and stiffened channels have opposite signs. In particular the load is decreasing along the equilibrium path if the displacement causes compression on the web (unstiffened channel: negative μ) or on the flanges (stiffened channels: positive μ). This can be explained from a mechanical point of view by considering that buckling is initiated by the web in unstiffened channels and the flanges in stiffened channels, respectively. Therefore any further displacement which increases pressure on the webs (in one case), or on the flanges (in the other case), is associated with a load decrement.

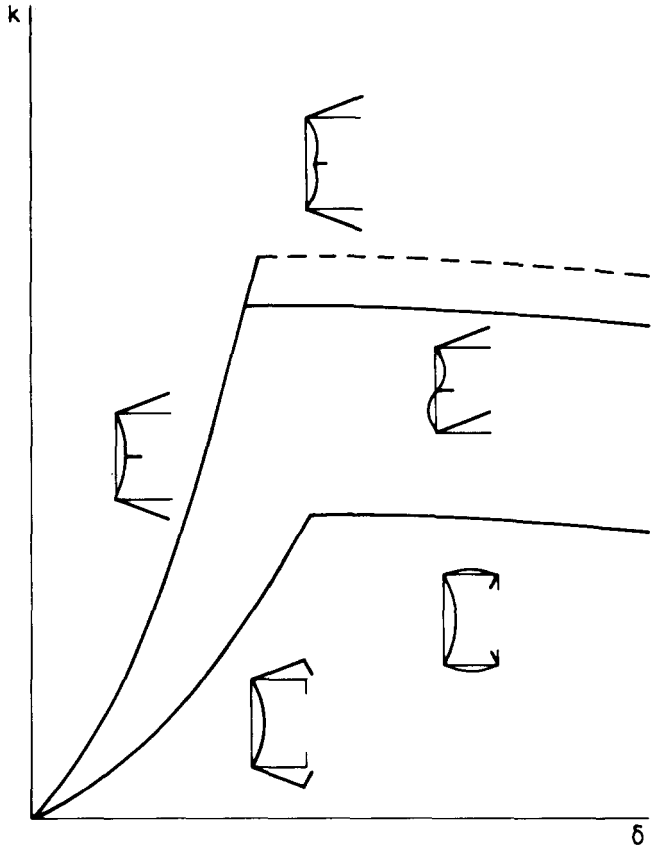

Fig. 5. Stiffened channel: critical stress versus stiffener rigidity.

TABLE 3
Web-stiffened Channel: E-local Interaction ($\beta = 0{\cdot}3, \gamma = 0{\cdot}01$)

	δ	α	c/h	$10^3\sigma_c/E$	ν_1	ν_2	μ	
							Eqn (5)	*Eqn (12)*
Loc.	0·00	14·2	1·09	0·393	0·630	±0·776	−0·734	−0·723
symm.	0·04	11·3	1·88	0·583	0·461	±0·887	0·630	0·625
	0·06	9·3	2·33	0·795	0·457	±0·890	1·352	1·316
Loc.	0·07	8·6	0·66	0·884	0·558	±0·830	14·560	14·600
antisymm.	0·10	8·5	0·65	0·885	0·557	±0·830	15·020	15·000

TABLE 4
Lipped Channel: E-local Interaction ($\beta = 0{\cdot}3$, $\gamma = 0{\cdot}01$)

	δ	α	c/h	$10^3\sigma_c/E$	ν_1	ν_2	μ	
							Eqn (5)	*Eqn (12)*
Loc. symm.	0·00	14·2	1·09	0·393	0·630	±0·776	−0·734	−0·723
	0·04	14·4	0·85	0·490	0·585	±0·811	−3·945	−3·903
	0·08	15·1	0·76	0·534	0·588	±0·808	−4·156	−4·172
	0·10	15·7	0·79	0·511	0·584	±0·812	−4·114	−4·090
	0·30	18·0	0·72	0·510	0·572	±0·820	−4·436	−4·365

Table 4 is concerned with the E-local interaction analysis of a lipped channel. It is to be noted that μ is always negative. This is in accord with previous explanation since buckling is initiated by compression webs. Note also that for increasing δ, μ rapidly approaches an asymptotic value which remains however much below the maximum observed in Table 3.

In both tables the last column collects results of the approximate analysis (eqns (12)). As in the previous case they are in good agreement with those obtained by solving the nonlinear eqns (5).

Finally in Fig. 6 the ultimate load λ_s versus the initial imperfections amplitude has been represented. It is clear that the most severe situation is determined by the simultaneous occurrence of Eulerian and local anti-symmetric buckling modes in web-reinforced channels since sensitivity to initial imperfections is more pronounced.

5.3 Stiffened channel: multiple interaction

A number of cases of multiple interaction have been investigated for stiffened channels. Due to the difficulties in solving nonlinear algebraic equations and encouraged by the good results previously obtained, use is made of the approximate equations (12).

Table 5 furnishes the coefficients A_{ijk} relative to the interaction between the Euler and two local symmetric buckling modes of a lipped channel sketched in the picture. It is seen that the two off-diagonal terms are very small in comparison with the main diagonal ones, due to the fact that the wavelengths of the two local modes are very different. This implies that the three modes interaction is weak in comparison with the two modes interaction.

Table 6 collects the A_{ijk}s relative to the interaction between the Euler and three local modes sketched in the picture of a web-reinforced channel. The

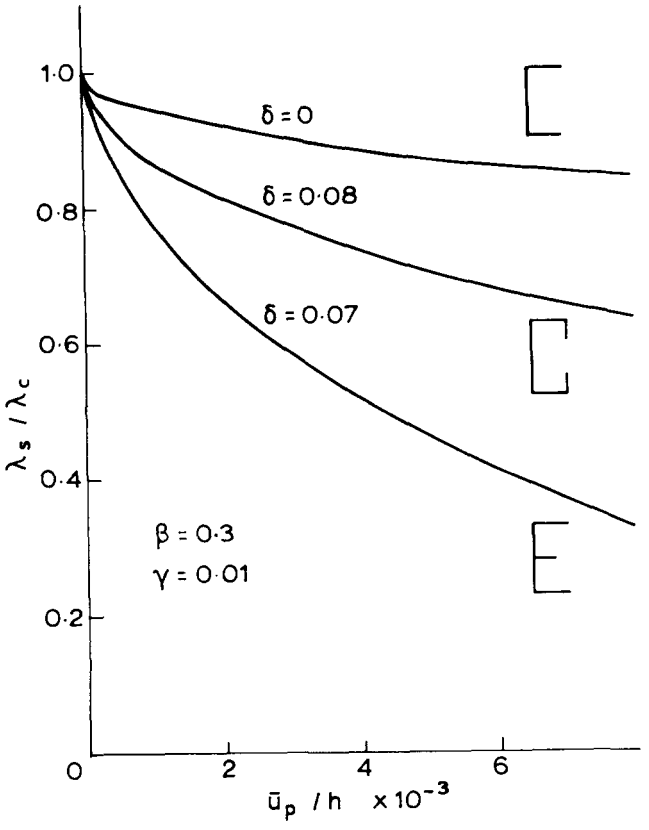

Fig. 6. Stiffened channel: snapping load versus initial imperfection amplitude.

TABLE 5
Lipped Channel: E-local Symm.–local Antisymm. Interaction
($\alpha = 30{\cdot}7, \beta = 0{\cdot}6, \gamma = 0{\cdot}01, \delta = 0{\cdot}065$)

j	A_{1jk}		*Local mode*	c/h
2	0·052	$0{\cdot}19\ 10^{-4}$		3·41
3	$0{\cdot}19\ 10^{-4}$	−0·038		0·88

TABLE 6
Web-stiffened Channel: E-local Symm.–local Antisymm. Interaction
($\alpha = 28{\cdot}6, \beta = 0{\cdot}6, \gamma = 0{\cdot}01, \delta = 0{\cdot}08$)

j	A_{1jk}			*Local mode*	c/h
2	0·018 0	−0·000 9	0	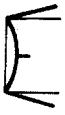	2·18
3		0·092 3	0		0·73
4	Symm.		0·092 1		0·73

TABLE 7
Web-stiffened Channel: FT—local Symm.–local Antisymm. Interaction
($\alpha = 28{\cdot}6, \beta = 0{\cdot}6, \gamma = 0{\cdot}01, \delta = 0{\cdot}08$)

j	A_{1jk}		*Local mode*	c/h
2	0	0·094		1·24
3	0·094	0		1·24

term A_{123} is much smaller than the main diagonal ones for the reasons illustrated above. Terms A_{124} and A_{134} vanish since interaction between a symmetric and an antisymmetric mode is involved. As a result there exists a single interaction between the Euler and the antisymmetric mode and a weak multiple interaction between the Euler and the two symmetric local modes. Both interactions are characterised by an approximately equal slope of the bifurcated paths.

Results relative to FT-local symmetric-local antisymmetric interaction for a web-reinforced channel are given in Table 7. In contrast with the two

previous results the dominant terms are the off-diagonal ones so that only multiple interaction occurs. This is due to the fact that the two local modes have the same wavelength. The slope of the bifurcated path $\mu = 9{\cdot}40$ is obtained having assumed as v_P the displacement of the point P in Fig. 1(b) in the Z-direction. Note that this value of μ is of the order of the largest ones obtained in the E-local interaction and therefore represents the same level of risk for the TWM.

6 CONCLUSIONS

On the basis of the general theory of elastic stability, third-order post-buckling analysis in the presence of two or more simultaneous buckling modes has been performed on TWM under uniform compression by means of the finite strip method. The initial imperfections effect is taken into account. An approximate procedure for the evaluation of v_i and λ_1 has been suggested which furnishes results in good agreement with the ones inherent to the solution of nonlinear algebraic equations. For cross-sections with an axis of symmetry this analysis allows prediction of situations in which interaction occurs by invoking purely geometric considerations. In contrast with results previously achieved it is found that flexural–torsional buckling may cause serious detrimental effects whenever interaction occurs between a local symmetric and an antisymmetric mode. A number of numerical results have been obtained for stiffened and unstiffened channels and an angle section which confirm the theoretical predictions.

The present analysis has to be completed by including fourth-order terms of the energy expansion in order to investigate postbuckling behaviour of TWM in cases where third order (asymmetric) interaction is weak.

REFERENCES

1. Koiter, W. T., Over de stabiliteit van het elastisch evenwicht (in Dutch), Ph.D. thesis H. J. Paris, Amsterdam 1945; English translation as NASA TTF-10, 833, 1967 and AFFDL Report TR 70-25, 1970.
2. Wang, S. T. and Pao, H. Y., Torsional–flexural buckling of locally buckled columns, *Int. J. Comp. Struct.*, **11** (1980).
3. Hancock, G. J., Interaction buckling in I-section columns, *Proc. ASCE*, **107**(ST1) (1981) 165–79.
4. Hancock, G. J., Nonlinear analysis of thin sections in compression, *Proc. ASCE*, **107**(ST3) (1981) 455–71.
5. Bradford, M. A. and Hancock, G. J., Elastic interaction of local and lateral buckling in beams, *Thin-Walled Struct.*, **2**(1) (1984) 1–25.

6. Byskov, E. and Hutchinson, J. W., Mode interaction in axially stiffened cylindrical shells, *AIAA J.*, **15**(7) (1977) 941–8.
7. Sridharan, S. and Benito, R., Columns: static and dynamic interactive buckling, *Proc. ASCE*, **110**(EM1) (1984) 49–65.
8. Benito, R. and Sridharan, S., Mode interaction in thin-walled structural members, *J. Struct. Mech.*, **12**(4) (1984–85), 517–42.
9. Sridharan, S., Doubly symmetric interactive buckling of plate structures, *Int. J. Solids Struct.*, **19**(7) (1983) 625–41.
10. Sridharan, S. and Ali, A., Interactive buckling in thin-walled beam columns, *Proc. ASCE*, **111**(EM12) (1985) 1470–86.
11. Pignataro, M., Luongo, A. and Rizzi, N., On the effect of the local-overall interaction on the postbuckling of uniformly compressed channels, *Thin-Walled Struct.*, **3** (1985) 293–321.
12. Byskov, E., Elastic buckling problem with infinitely many local modes, Rep. No. 327, Technical University of Denmark, Lyngby, Denmark, 1986.
13. Pignataro, M. and Luongo, A., Multiple interactive buckling of thin-walled members in compression, *Proc. Int. Colloq. on Stability of plate and shell structures*, Ghent, 1987.
14. Budiansky, B., Theory of buckling and postbuckling behaviour of elastic structures, In *Advances in Applied Mechanics*, Vol. 14 (Chia-Shun Yih, ed.), New York, Academic Press, 1974.
15. Luongo, A. and Pignataro, M., Buckling and post-buckling analysis of stiffened channels under uniform compression, *Costruzioni Metalliche*, **4** (1986) 242–9.